Tunneling conductance and local density of states in time-reversal symmetry breaking superconductors under the influence of an external magnetic field

Mihail A. Silaev,[1] Takehito Yokoyama,[2] Jacob Linder,[3] Yukio Tanaka,[2] and Asle Sudbø[3]
[1]*Institute for Physics of Microstructures, Russian Academy of Sciences, 603950 Nizhny Novgorod GSP-105, Russia*
[2]*Department of Applied Physics, Nagoya University, Nagoya, 464-8603, Japan and CREST, Nagoya, 464-8603, Japan*
[3]*Department of Physics, Norwegian University of Science and Technology, N-7491 Trondheim, Norway*
(Received 1 November 2008; published 10 February 2009)

We consider different effects that arise when time-reversal symmetry breaking superconductors are subjected to an external magnetic field, thus rendering the superconductor to be in the mixed state. We focus in particular on two time-reversal symmetry breaking order parameters which are believed to be realized in actual materials: $p+ip'$ wave and $d+is$ or $d+id'$ wave. The first-order parameter is relevant for Sr_2RuO_4, while the latter order parameters have been suggested to exist near surfaces in some of the high-T_c cuprates. We investigate the interplay between surface states and vortex states in the presence of an external magnetic field and their influence on both the tunneling conductance and the local density of states. Our findings may be helpful to experimentally identify the symmetry of unconventional time-reversal symmetry breaking superconducting states.

DOI: 10.1103/PhysRevB.79.054508 PACS number(s): 74.45.+c, 74.20.Rp, 74.25.−q

I. INTRODUCTION

Recently, considerable attention has been devoted to the chiral superconducting phase which is believed to be realized in the p-wave triplet superconductor[1] Sr_2RuO_4. The chiral state of a p-wave superconductor corresponds to a nonzero projection $l_z=\pm 1$ of the Cooper pairs angular momentum $\mathbf{l}$ along the z axis, and thus breaks time-reversal symmetry (TRS). The spatially homogeneous triplet order parameter (OP) $\hat{\Delta}=\Delta_0(\mathbf{d}\cdot\hat{\sigma})i\hat{\sigma}_y$ is described by the vector[1] $\mathbf{d}(\mathbf{p})=(0,0,p_x+i\chi p_y)$, which depends on the direction of electron momentum $\mathbf{p}$. Here Δ_0 is the bulk value of the order parameter, $\hat{\sigma}=(\hat{\sigma}_x,\hat{\sigma}_y,\hat{\sigma}_z)$ is the vector of Pauli matrices of conventional spin operators, and $\chi=\pm 1$ corresponds to the two possible values of chirality. Also, chiral superconducting states can be associated with an admixture of two order parameters corresponding to different irreducible representations of crystal point group. Different order parameter components can naturally coexist in the vicinity of interfaces between superconductors and surfaces due to the broken symmetry of the crystal group.[2–5] Among the possibilities of subdominant order parameter symmetries,[2] there are states which break time-reversal symmetry.[3–5] The coexistence of order parameters shows up in the local density of states,[6–9] as well as in the generation of spontaneous currents flowing along the surfaces in the time-reversal symmetry breaking cases.[7,8]

Time-reversal symmetry breaking order parameters have been proposed to exist near surfaces[10] and within vortex cores[11] in high-T_c superconductors. This proposal stems from the observation of a split zero-bias conductance peak in the *absence* of any applied magnetic field. In this case, it has been suggested that the relevant order parameter is either $d+is$ or $d+id'$ wave. The gap may then be written as $\Delta=\Delta_0 g(\theta_p)+i\Delta_s$ or $\Delta=\Delta_0 g(\theta_p)+i\Delta_d g_1(\theta_p)$, respectively, where Δ_0 is an amplitude of the main component and the admixture of another pairing symmetry is denoted by the amplitudes Δ_s and Δ_d. Here, θ_p is a polar angle in momentum space $\mathbf{p}=p(\cos\theta_p,\sin\theta_p)$; $g(\theta_p)=\cos(2\theta_p+\alpha)$ and $g_1(\theta_p)=\sin(2\theta_p+\alpha)$, where $\alpha/2$ is an angle measuring the disorientation of crystalline symmetry axes and coordinate axes. One obtains $d_{x^2-y^2}$-wave symmetry of the main order-parameter component for $\alpha=0$ and d_{xy}-wave pairing for $\alpha=\pi/2$. While the experimental data so far clearly indicate an order parameter which breaks time-reversal symmetry, the question of whether the symmetry is $d+is$ or $d+id'$ wave remains unsolved. Clearly, experimental signatures that may distinguish these two types of pairings would be highly desirable.

One of the important features of unconventional superconductors is the possibility for the existence of surface Andreev bound states.[12–14] They occur in the vicinity of the scattering interface between a superconductor and an insulator if the incident and reflected quasiparticles (QPs) with different momentum directions see different phases of the order parameter. The consequence of the Andreev bound-state formation is an increase in the local density of states (DOS) (LDOS) at the surface resulting in zero-bias conductance peak anomaly observed[15] in tunneling spectroscopy of high-T_c cuprates with d-wave symmetry of superconducting pairing as well as in the p-wave triplet superconductor Sr_2RuO_4.[16] Also, the Andreev bound states determine the anomalous low-temperature behavior of the London penetration length[17] and the Josephson critical current in d-wave[18] and chiral superconductors.[19]

Under the influence of an applied magnetic field, screening currents and vortices may be generated in a superconductor. As a result, the spectrum of surface states acquires a Doppler shift, leading to a splitting of the zero-bias conductance peak.[10] Abrikosov vortices located near a superconducting surface generate an essentially inhomogeneous superfluid velocity field, which leads to a nontrivial electronic structure of the surface-bound states.[20–22] Also, it was recently[22] proposed that the same Doppler-shift effect should lead to a chirality-selective influence of the magnetic field on the surface states in a p-wave chiral superconductor with broken time-reversal invariance. The quasiparticle DOS near

a flat surface was shown to depend on the orientation of magnetic field with respect to the chirality as well as on the vorticity in the case where the Abrikosov vortex is pinned near the surface of superconductor. Additionally, in superconductors featuring gap nodes, such as in the case in pure $d_{x^2-y^2}$-symmetric superconducting cuprates, a vanishing pair potential in nodal directions results in important ramifications for the physics of the system.[11,23–26]

To understand the effect of an externally applied magnetic field on the surface DOS, let us consider a spectrum of Andreev bound states near a flat surface of a time-reversal symmetry breaking superconductor occupying the half-space $x>0$. Below, we focus on the $p+ip$-, $d_{xy}+is$-, and $d_{xy}+id_{x^2-y^2}$-wave cases for concreteness. We consider a model situation assuming spatially homogeneous gap function, having the following form in momentum space:

$$\Delta = \Delta_0 e^{i\chi\theta_p} \tag{1}$$

for $p+ip$-wave,

$$\Delta = \Delta_0 \sin(2\theta_p) + i\Delta_s \tag{2}$$

for $d_{xy}+is$-wave, and

$$\Delta = \Delta_0 \sin(2\theta_p) + i\Delta_d \cos(2\theta_p) \tag{3}$$

for $d_{xy}+id_{x^2-y^2}$-wave superconductors.

Assuming that the QPs are specularly reflected at the surface of the superconductor within a Doppler-shift approach,[27] the spectrum of the surface states can be expressed as follows:[19,28] $\varepsilon_a=\varepsilon_{a0}+\epsilon_D$, where ε_{a0} is a position of energy level in zero magnetic field and $\epsilon_D=\hbar\mathbf{k}_F\mathbf{v}_s$ is the Doppler-shift energy which is determined by a local field of superfluid velocity. The superfluid velocity $\mathbf{v}_s$ near a surface has only a tangential component, directed along the y axis $\mathbf{v}_s=(0,v_{sy},0)$, and can be related to the density of supercurrent flowing along the surface $\mathbf{j}_s=en\mathbf{v}_s$, where e is the electron charge and n is the concentration of Cooper pairs. The magnetic field is screened in a superconductor at the London length λ as follows: $B=He^{-x/\lambda}$, where H is the value of magnetic field outside the superconductor. Therefore, the superfluid velocity is $v_{sy}=-(2e/mc)\lambda H$.

If the magnetic field is absent, the spectrum of surface states is given by[12,29]

$$\varepsilon_{0a} = \chi\Delta_0 k_y/k_F \tag{4}$$

for a chiral p wave,

$$\varepsilon_{a0} = \Delta_s \,\mathrm{sgn}(k_y) \tag{5}$$

for a $d_{xy}+is$ wave, and

$$\varepsilon_{a0} = \Delta_d \,\mathrm{sgn}(k_y)\cos(2\theta_p) \tag{6}$$

for a $d_{xy}+id_{x^2-y^2}$ wave. Here k_y is the projection of QP momentum along the surface. The above spectra may be formally obtained by solving[13]

$$\frac{\Delta(\theta_p)}{\varepsilon_{a0}-i\sqrt{|\Delta(\theta_p)|^2-\varepsilon_{a0}^2}} = \frac{\Delta(\pi-\theta_p)}{\varepsilon_{a0}+i\sqrt{|\Delta(\pi-\theta_p)|^2-\varepsilon_{a0}^2}}. \tag{7}$$

In the $d_{x^2-y^2}+is$-wave case, one finds that $\varepsilon_{a0}=\sqrt{\Delta_0^2\cos^2(2\theta_p)+\Delta_s^2}$, from which one infers that there are no subgap surface states. This is qualitatively different from the $d_{xy}+is$-wave case. The interesting effects occur in the latter case, so we focus on the $d_{xy}+is(d)$-wave symmetry in the following, corresponding to $\alpha=\pi/2$.

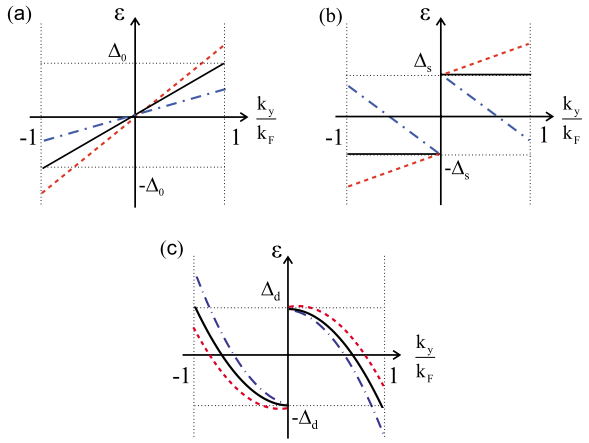

FIG. 1. (Color online) Plot of the surface states spectrum for (a) chiral $p+ip$-wave, (b) $d+is$-wave, and (c) $d+id$-wave superconductors. Spectrum in zero magnetic field is shown by solid lines. Blue (dash-dotted) and red (dotted) lines correspond to the spectrum transformation due to magnetic field directed along and opposite the z axis correspondingly.

The transformation of these spectra due to the Doppler-shift effect is shown in Fig. 1. To be definite we assume that $\Delta_s>0$, $\Delta_d>0$, and $\chi=1$. Considering the DOS at Fermi level, $\nu=|\partial\varepsilon_a/\partial k_y|^{-1}_{\varepsilon=0}$, in a chiral p-wave superconductor one can see that its dependence on the magnetic field is monotonic: it either increases or decreases for different field directions [see Fig. 1(a)] as discussed in Ref. 22.

Another behavior of the DOS occurs in the case of a $d+is$-wave superconductor. From Fig. 1(b) it follows that for a certain field direction there are no states at the Fermi level $\varepsilon=0$ [red dashed lines in Fig. 1(b)]. For the opposite field direction [blue dashed-dotted lines in Fig. 1(b)], intersections of spectral branches with the Fermi level appear when the superfluid velocity is large enough, $|v_{sy}|>\Delta_s/p_F$, so that the value of momentum projection at the intersection point is smaller than the Fermi momentum $|k_y^*|<k_F$. Thus, one can expect that the DOS at the Fermi level should be zero when $H<H^*$, where H^* is the magnetic field value providing the condition $|v_{sy}|=|\Delta_s|/p_F$ to be fulfilled.

On the contrary, in the $d+id$-wave case the DOS at the Fermi level is nonzero even in the absence of a magnetic field. As can be seen from Fig. 1(c) (black solid lines) the spectral branches intersect the level $\varepsilon=0$ at $k_y^*=\pm k_F/\sqrt{2}$. The transformation of the spectrum due to the magnetic field of different directions is shown in Fig. 1(c) by red dashed lines ($H>0$) and by blue dashed-dotted lines ($H<0$). Then, it can be easily seen that for $H>0$ the coordinates of the intersection points k_y^* shift toward $\pm k_F$ and for a certain value of the magnetic field $H>H^*$ the DOS at the Fermi level $\varepsilon=0$ disappears.

In the presence of an Abrikosov vortex near the surface of chiral superconductor a nontrivial structure of the local density of states distribution appears which depends on the vor-

tex orientation.[22] Along with the Doppler-shift effect,[22] an important modification of the quasiparticle spectrum and the DOS can be obtained due to the overlapping of the surface states and the low-energy QP states localized within the vortex core found in the pioneering work by Caroli, de Gennes, and Matricon (CdGM).[30] It was shown that QP states with energy lower than the bulk superconducting gap value Δ are localized within the vortex core at the characteristic scale of the order of coherence length ξ and have a discrete spectrum $\varepsilon_v(\mu)$ as a function of the quantized (half-integer) angular momentum μ. At small energies $|\varepsilon| \ll \Delta$ the spectrum for a vortex with vorticity M is given by

$$\varepsilon_v(\mu) \approx -M\mu\omega, \tag{8}$$

where $k_F = p_F/\hbar$ and $\omega \sim \Delta_0/k_F\xi$. For most of superconducting materials, including Sr_2RuO_4, the interlevel spacing ω is much less than the superconducting gap Δ since $k_F\xi \gg 1$. Therefore, the CdGM spectrum may be considered as a continuous function of the impact parameter of the quasiclassical trajectory $b=-\mu/k_F$ and the direction of QP momentum θ_p as in the following form:

$$\varepsilon_v(b, \theta_p) \approx M\Delta(b/\xi). \tag{9}$$

In the case of a chiral p-wave superconductor, the spectrum of vortex core states differs from the CdGM result and is given by Eq. (8) with integer μ. For the $d+is$- and $d+id$-wave superconductors the quasiclassical spectrum of vortex core states is given by Eq. (9) with $\Delta(\theta_p) = \sqrt{\Delta_0^2 g^2(\theta_p) + \Delta_s^2}$ and $\Delta(\theta_p) = \sqrt{\Delta_0^2 g^2(\theta_p) + \Delta_d^2 g_1^2(\theta_p)}$. The discrete spectrum is obtained by applying the Bohr-Sommerfeld quantization rule to the canonical variables $\mu=-k_F b$ and θ_p.[23,31] It should be noted that when the superconducting order parameter contains nodes, the quasiclassical expression (9) is invalid near the nodal directions since energy states near the vortex core are not truly localized but rather "leak" out through the gap nodes.[11,23–26] This is not the case for us since we consider superconducting order parameters which are gapped over the entire Fermi surface.

To study the interaction between vortex and surface states, let us consider an example of vortex positioned near a flat surface of chiral $p+ip$-wave superconductor. Comparing the energies of surface ε_a (4) and vortex ε_v (9) states one can see that for certain QP trajectories the condition of resonance $\varepsilon_a = \varepsilon_v$ is realized. Thus the spectrum transformation in such almost degenerate two-level system is given by a secular equation

$$(\varepsilon - \varepsilon_a)(\varepsilon - \varepsilon_v) = J^2. \tag{10}$$

Since we consider a low-energy spectrum $|\varepsilon| \ll \Delta_0$, the trajectories should pass close to the vortex center for the spectrum modification (10) to be effective. Then, the interaction of surface and vortex states is determined by the overlap integral $J \approx \Delta \exp(-\tilde{a}/\xi)$, where $\tilde{a} = a/\cos\theta_p$ and a is the distance from the vortex to the surface. Taking a certain point at the surface [see point A in Fig. 2(a)] of the superconductor one can obtain a relation between the angles and impact parameters of trajectories passing through this point as follows: $b = \tilde{a}\sin(\theta - \theta_p)$. Thus the energy of vortex core states can be written as $\varepsilon_v = M(\tilde{a}/\xi)\Delta_0 \sin(\theta - \theta_p)$. Then, from Eq. (10) we

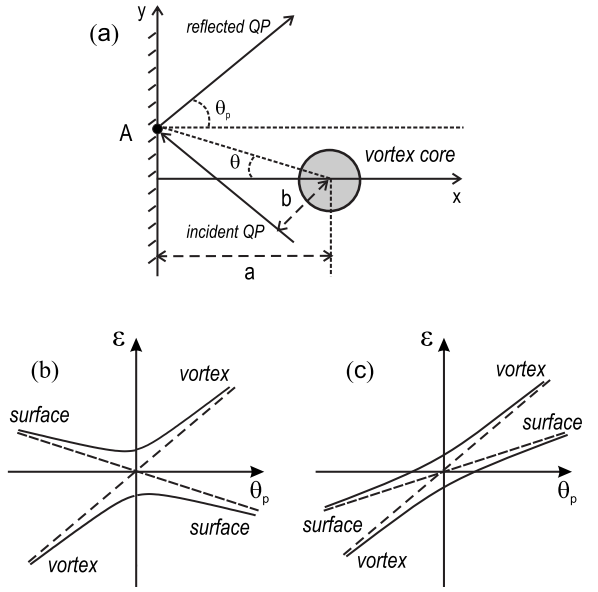

FIG. 2. (a) Sketch of QP trajectories forming surface and vortex states and qualitative plot of spectrum transformation due to the interaction of surface and vortex states in the case of a chiral p-wave superconductor; vorticity and chirality have (b) equal and (c) opposite values.

obtain the spectrum transformation shown qualitatively in Fig. 2 for the particular case of $\theta=0$. It is easy to see that for equal values of vorticity and chirality [Fig. 2(b)] there appears a minigap in quasiparticle spectrum near the Fermi level and therefore the zero-energy DOS is suppressed. On the other hand, in the case of opposite vorticity and chirality [Fig. 2(c)] there is no minigap and the DOS is not suppressed.

In $d+is$- and $d+id$-wave superconductors, the interaction between vortex and surface states can also lead to noticeable effects, which will be discussed later in the present paper. Recently, it was pointed out that tunneling of quasiparticles into vortex core states leads to a resonant enhancement of subgap conductance of normal-metal/superconductor (N/S) junction.[32] In the case of chiral superconductors, such a tunneling effect can lead to either stimulation or suppression of conductance, depending on the direction of vorticity. We will show that if vortices are located far from the N/S interface, the conductance follows the behavior expected from the Doppler-shift approach. On the other hand, when the distance from the vortex to the interface becomes comparable with coherence length ξ the tunneling into vortex core states comes into play, leading to the peculiar nonmonotonic conductance dependence on the vortex coordinate with respect to the superconducting surface.

This paper is organized as follows. In Sec. II, we give an overview of the theoretical framework which is employed in this work, namely, a Bogoliubov approach and a quasiclassical Eilenberger approach. In Sec. III, we present our main results for the influence of magnetic field on bound surface states spectra and local density of states near the surface. We discuss the transformation of surface states in the Meissner state of superconductor as well as the effects of interplay between surface and vortex core states. We give our conclusions in Sec. IV.

II. THEORETICAL APPROACH

Our further considerations are based on the Bogoliubov–de Gennes (BdG) equations for particlelike (u) and holelike (v) parts of the wave function, which have the following form:

$$-\frac{1}{2m}\left(\hat{\mathbf{p}}-\frac{e}{c}\mathbf{A}\right)^2 u+\hat{\Delta}v=(\varepsilon+\varepsilon_F)u,$$

$$\frac{1}{2m}\left(\hat{\mathbf{p}}+\frac{e}{c}\mathbf{A}\right)^2 v+\hat{\Delta}^{\dagger}u=(\varepsilon-\varepsilon_F)v. \tag{11}$$

Here $\hat{\Delta}$ is the gap operator, $\mathbf{A}$ is the vector potential, $\hat{\mathbf{p}}=-i(\partial/\partial_x,\partial/\partial_y)$, and $\mathbf{r}=(x,y)$ is the radius vector in the plane perpendicular to the anisotropy plane. Hereafter we assume the Fermi surface to be cylindrical along the z axis and consider a motion of QPs only in xy plane.

In the case of unconventional superconductors, the gap potential $\hat{\Delta}$ is a nonlocal operator, so the BdG system effectively becomes a very complicated integrodifferential equation. Another complexity arises from the broken spatial invariance of the superconducting gap in the presence of vortices near the N/S interface. A simplification can be obtained if one considers a quasiclassical approximation, assuming that the wavelength of quasiparticles is much smaller than the superconducting coherence length (see, e.g., Ref. 33). Within such an approximation, QPs move along linear trajectories, i.e., straight lines along the direction of QP momentum $\mathbf{n}=\mathbf{k}_F k_F^{-1}=(\cos\theta_p,\sin\theta_p)$. Generally, the quasiclassical form of the wave function can be constructed as follows: $(u,v)=e^{i\mathbf{k}_F\mathbf{r}}(U,V)$, where $(U(\mathbf{r}),V(\mathbf{r}))$ is a slowly varying envelope function. Then system (11) reduces to a system of first-order differential equations along the linear trajectories defined by the direction of the QP momentum $\mathbf{n}=\mathbf{k}_F k_F^{-1}=(\cos\theta_p,\sin\theta_p)$. Introducing the coordinate along trajectory $x'=(\mathbf{n}\cdot\mathbf{r})=r\cos(\theta_p-\theta)$, we arrive at the following form of the quasiclassical equations:

$$\left(-i\hbar v_F\partial_{x'}+\mathbf{v}_F\cdot\frac{e}{c}\mathbf{A}\right)U+\Delta V=\varepsilon U,$$

$$\left(i\hbar v_F\partial_{x'}+\mathbf{v}_F\cdot\frac{e}{c}\mathbf{A}\right)V+\Delta^{\dagger}U=\varepsilon V, \tag{12}$$

where the Fermi velocity is $\mathbf{v}_F=\mathbf{n}\hbar k_F/m$. The pairing potential in Eq. (12) may generally be written as

$$\Delta(\mathbf{r},\theta_p)=\Delta(\theta_p)\Psi(\mathbf{r}), \tag{13}$$

where $\Delta(\theta_p)$ describes the orbital symmetry of the superconducting order parameter in momentum space, while $\Psi(\mathbf{r})$ describes its spatial dependence both magnitudewise and phasewise.

The LDOS can be expressed through the eigenfunctions of the BdG equation (11) in the following form:[34]

$$N(\varepsilon,\mathbf{r})=\sum_n |u_n(\mathbf{r})|^2\delta(\varepsilon-\varepsilon_n), \tag{14}$$

where $u_n(\mathbf{r})$ is electron component of quasiparticle eigenfunction corresponding to an energy level ε_n. The eigenfunction has to be normalized; $\int\int_{-\infty}^{\infty}|u_n(\mathbf{r})|^2+|v_n(\mathbf{r})|^2d^2r=1$.

We will also later employ the quasiclassical Eilenberger approach to study the spatially resolved DOS. Let us here sketch the framework of the treatment which makes use of the Eilenberger equation, following the notation of Refs. 35 and 36. It is now convenient to solve the Eilenberger equation along trajectories along the Fermi momentum and to introduce a Ricatti parametrization for the Green's function.[36] In this way, one obtains[20]

$$\hbar v_F\partial_{x'}a(x')+[2\tilde{\omega}_n+\Delta^{\dagger}a(x')]a(x')-\Delta=0,$$

$$\hbar v_F\partial_{x'}b(x')-[2\tilde{\omega}_n+\Delta b(x')]b(x')+\Delta^{\dagger}=0, \tag{15}$$

where $i\tilde{\omega}_n=i\omega_n+m\mathbf{v}_F\cdot\mathbf{v}_s$ is a Doppler-shifted Matsubara frequency and

$$\mathbf{v}_s=\frac{1}{2m}\left(\hbar\nabla\Phi-\frac{2e}{c}\mathbf{A}\right)$$

is a gauge-invariant superfluid velocity where $\Phi(\mathbf{r})$ is a gap function phase; $\Psi(\mathbf{r})=|\Psi|e^{i\Phi}$. The LDOS may be expressed through the scalar coherence functions a and b as follows:[20]

$$N(\varepsilon)=\int_0^{2\pi}\frac{d\theta}{2\pi}\mathrm{Re}\left\{\frac{1-ab}{1+ab}\right\}_{i\omega_n\to\varepsilon+i\delta}, \tag{16}$$

where ε is the quasiparticle energy measured from Fermi level and δ is a scattering parameter which accounts for inelastic scattering.

To investigate the transport properties of N/S junction, we employ an approach similar to what was used in work by Blonder *et al.*[37] The expression for the dimensionless zero-bias conductance of the N/S junction measured in terms of the conductance quantum $e^2/\pi\hbar$ can be written as follows:

$$G=\frac{G_{\mathrm{Sh}}}{2}\int_{-\pi/2}^{\pi/2}[1-R_n(\theta_0)+R_a(\theta_0)]\cos\theta_0 d\theta_0, \tag{17}$$

where $R_n(\theta_0)$ and $R_a(\theta_0)$ are the probabilities of normal and Andreev reflections respectively, θ_0 is the incident angle, $\mathbf{k}_F=k_F(\cos\theta_0,\sin\theta_0)$, characterizing the propagation direction of quasiparticles coming from the normal-metal region. The Sharvin conductance $G_{\mathrm{Sh}}=k_F L_y/\pi$ equals the total number of propagating modes determined by the channel width L_y.

The problem of quasiparticle scattering at the N/S interface is formulated within the BdG theory (11).[38] An interfacial barrier separating the N and S regions can be modeled by repulsive delta function potential $W(x)=W_0\delta(x)$ parametrized by a dimensionless barrier strength $Z=W_0/\hbar v_F$. The boundary conditions at the N/S interface then read[39]

$$[f(0)]=0,\quad [\partial_x f(0)]=2k_F Z f(0), \tag{18}$$

where $f=(u,v)$ and $[f(x)]=f(x+0)-f(x-0)$.

Considering a zero-bias problem we will have to analyze only zero-energy excitations with $\varepsilon=0$. For wave functions in S region corresponding to subgap quasiparticles, the following representation can be used: (U,V)

$=e^{\zeta}(e^{i(\eta+\Phi)/2}, e^{-i(\eta+\Phi)/2})$, where $\zeta=\zeta(s,b)$ and $\eta=\eta(s,b)$ are real-valued functions. Then, the quasiclassical equation (12) can be written as follows:

$$\partial_{x'}\eta + 2|\Delta|\cos\ \eta + 2\epsilon_D = 0,$$

$$\partial_{x'}\zeta + 2|\Delta|\sin\ \eta = 0. \tag{19}$$

where $\epsilon_D(\mathbf{r})=\hbar\mathbf{k}_F\mathbf{v}_s$ is the Doppler-shift energy. For wave functions decaying at the different ends of trajectory $(U,V)(x'=\pm\infty)=0$ from Eq. (19) we obtain

$$\eta(x'=\pm\infty)=\pm\pi/2. \tag{20}$$

The boundary conditions (18) model the specularly reflecting N/S interface, coupling the waves with wave vectors $\mathbf{k}_F=k_F(\cos\theta_0,\sin\theta_0)$ and $\mathbf{k}'_F=k_F[\cos(\pi-\theta_0),\sin(\pi-\theta_0)]$. Therefore if the incident electron wave is $u_i=e^{i\mathbf{k}_F\cdot\mathbf{r}}$, then the reflected electron u_r and hole v_r waves will have the form

$$u_r = U_r e^{i\mathbf{k}'_F\cdot\mathbf{r}}, \quad v_r = V_r e^{i\mathbf{k}_F\cdot\mathbf{r}},$$

where U_r and V_r are the envelope functions. Thus, each point $(0,y)$ at the N/S interface lies on the intersection of two quasiclassical trajectories characterized by the angles $\theta_p=\theta_0$ and $\theta_p=\pi-\theta_0$. Let us denote the distribution of phases $\eta(x')$ along these trajectories as $\eta_+(x')$ and $\eta_-(x')$ correspondingly. Using the boundary conditions we obtain the following expression for the conductance:[32]

$$G = \frac{N_0}{2}\int_{-L_y/2}^{L_y/2}\int_{-\pi/2}^{\pi/2} g(y,\theta_0)\cos\ \theta_0 d\theta_0 dy, \tag{21}$$

where $g(y,\theta_0)$ is given by

$$g(y,\theta_0) = \frac{2}{(\tilde{Z}^4+\tilde{Z}^2)|1-e^{i\rho}|^2+1} \tag{22}$$

with $\tilde{Z}=Z/\cos\ \theta_0$ and $\rho(y,\theta_0)=\eta_--\eta_+$ is determined by the difference of phases $\eta_-(x')$ and $\eta_+(x')$ at the intersection point $(0,y)$. To evaluate the conductance, one needs to find the factor $e^{i\rho}$ in Eq. (22) and then the reflection probabilities by solving numerically Eq. (19) with the boundary conditions in Eq. (20).

III. RESULTS

To illustrate the basic effect of how the interplay between the Doppler shift and the time-reversal symmetry breaking of the superconducting order parameter is manifested, we consider a situation where an external magnetic field is applied near the surface of the superconductor along the $\hat{\mathbf{z}}$ axis, thus inducing a vector potential $\mathbf{A}$ in the superconductor which drives the shielding supercurrent. In order to proceed analytically, we make the simplifying assumption that the superfluid velocity field is nearly homogeneous and that the spatial variation in the superconducting order parameter near the interface is small. Choosing a real gauge, we then find that the Ricatti functions a and b in Eq. (15) may be written as[20,22]

$$a(\theta)=s(\theta)\Delta(\theta), \quad b(\theta)=s(\theta)\Delta^*(\theta),$$

$$s(\theta)=1/\{\tilde{\omega}_n(\theta)+\sqrt{[\tilde{\omega}_n(\theta)]^2+|\Delta(\theta)|^2}\}, \tag{23}$$

where $\tilde{\omega}_n$ depends on θ through the Doppler shift. To evaluate the LDOS in Eq. (16) at the surface, we need to take into account proper boundary conditions at $x=0$. Assuming an impenetrable surface with perfect reflection, these boundary conditions read

$$a_{\text{surface}}(\theta)=a(\pi-\theta), \quad b_{\text{surface}}(\theta)=b(\theta). \tag{24}$$

Inserting these into the expression for the LDOS, we obtain

$$N(\varepsilon)=2\ \text{Re}\left\{\left\langle\frac{1}{1+a(\pi-\theta)b(\theta)}\right\rangle\right\}_{i\omega_n\to\varepsilon+i\delta}-1. \tag{25}$$

$\langle\cdots\rangle$ denotes angular averaging, which we restrict to angles $-\pi/2\le\theta\le\pi/2$ due to the surface. It may be shown that, for a chiral p-wave superconductor,[22] the zero-energy DOS at the surface reads

$$N(0)=1+\frac{\hbar k_F v_{sy}}{\Delta_0}+\cdots, \tag{26}$$

while for pure s- or d-wave superconductors one finds

$$N(0)=C_1+C_2 v_{sy}^2+\cdots, \tag{27}$$

where C_1 and C_2 are arbitrary constants. From numerical investigations of Eq. (25) at $\varepsilon=0$, we find that the zero-energy DOS may quite generally be written as

$$N(0)=C_1+C_2 v_{sy}+\cdots \tag{28}$$

whenever the superconducting order parameters (i) break time-reversal symmetry and (ii) support the presence of subgap surface-bound states. This is the case both for the p_x+ip_y-wave pairing which is believed to be realized in Sr_2RuO_4, as well as the $d+is$-wave and $d+id$-wave pairings that are relevant for the cuprates. In particular, tunneling spectroscopy measurements have indicated the presence of such a time-reversal symmetry breaking order parameter near surfaces by a split zero-bias conductance peak that was observed in the *absence* of an external field in several experiments.[10]

In Ref. 35, it was pointed out that the neglect of the gradient term in the Eilenberger equation is expected to be a reasonable approximation as long as the Doppler-shift energy $m\mathbf{v}_F\cdot\mathbf{v}_s$ is small compared to the local gap energy $\Delta(\theta)$. This approximation would then fail close to the vortex core or gap nodes of $\Delta(\theta)$. Nevertheless, in the model case of spatially homogeneous gap function and superfluid velocity field, the gradient terms in the —Eilenberger equation can be neglected in the whole range of Doppler-shift energies. However considering a model situation the above discussion nevertheless serves to illustrate our main qualitative argument, namely, that chirality-sensitive effects should be expected in superconductors with order parameters that (i) break time-reversal symmetry and (ii) support the presence of subgap surface-bound states. We now proceed to discuss the cases of p_x+ip_y-wave and $d+is(d)$-wave pairings in more detail since these are relevant to actual materials.

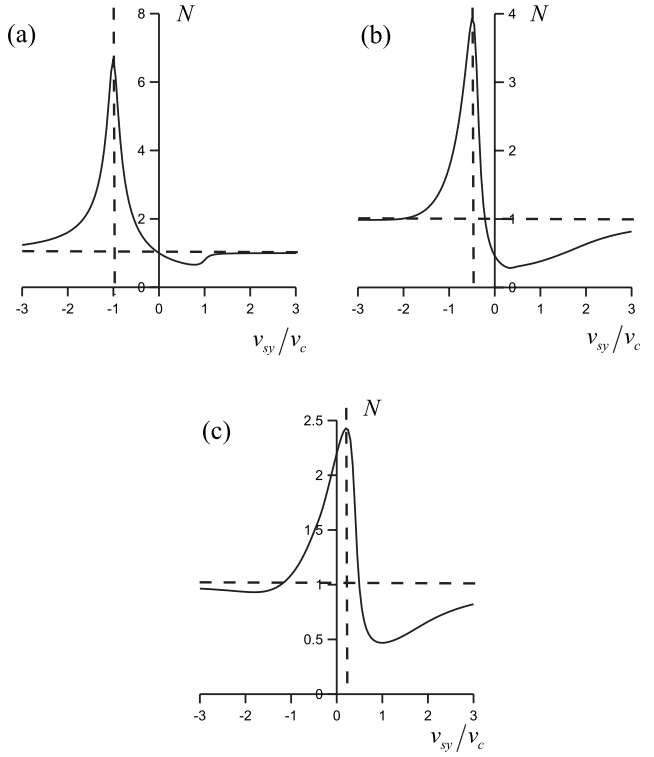

FIG. 3. Plot of the normalized zero-energy LDOS $N(0)$ for (a) p-wave superconductor with $\chi=1$, (b) $d+is$-wave case with $\Delta_s=0.4\Delta_0$, and (c) $d+id$-wave case with $\Delta_d=0.4\Delta_0$. Dashed lines are guides for eyes. The vertical ones denote positions of LDOS peaks and the horizontal ones correspond to the level of normal-metal DOS N_0.

A. Surface states in $p+ip$ and $d+is(d)$ superconductors under the influence of magnetic field

In Fig. 3, we show numerical plots of the surface LDOS given by Eq. (25) for the chiral p-wave [Fig. 3(a)], $d+is$-wave [Fig. 3(b)], and $d+id$-wave [Fig. 3(c)] cases in a wide domain of superfluid velocities. The structure of gap functions is chosen in the form of Eqs. (1)–(3) and the parameter characterizing inelastic scattering in Eq. (16) is chosen as $\delta=0.1\Delta_0$. We introduce the following notations for the different critical velocities: $v_c=\Delta_0/\hbar k_F$, $v_{cs}=|\Delta_s|/\hbar k_F$ and $v_{cd}=|\Delta_d|/\hbar k_F$.

As seen, the surface LDOS has sharp peaks at a certain value of the superfluid velocity in all cases. We will show below that peaked structure of LDOS is provided by bound surface states. Another contribution to the LDOS comes from the delocalized states corresponding to the continuous part of QP spectrum. A delocalized state with zero energy $\varepsilon=0$ exists provided that (i) $|v_{sy}|>v_c$ in case of chiral p-wave superconductor and (ii) $|v_{sy}|>v_{cs}$ and (iii) $|v_{sy}|>v_{cd}$ in cases of $d+is$-wave and $d+id$-wave superconductors correspondingly. Condition (i) is unlikely to be realized because it means that the superfluid velocity is larger than the critical depairing value. Conditions (ii) and (iii) can be realized because the values v_{cs} and v_{cd} can be well below the critical depairing velocity if the amplitude of additional order-parameter components is small enough.

To analyze the contribution to LDOS provided by the bound surface states we will consider the domain of low energies $|\varepsilon|\ll\Delta_0$. By neglecting small deviations of the electron and hole momenta, the normalized wave function of QP localized near the boundary can be written as

$$\begin{pmatrix} u \\ v \end{pmatrix} = \begin{pmatrix} 1 \\ i \end{pmatrix} \sqrt{\frac{2}{\tilde{\xi}|\cos\theta_p|}} e^{ik_y y} \sin(k_x x) e^{-x/(\tilde{\xi}\cos\theta_p)},$$

where $(k_x,k_y)=k_F(\cos\theta_p,\sin\theta_p)$. This wave-function decay in the superconducting side $x>0$ at a characteristic localization scale $\tilde{\xi}$ is given by $\tilde{\xi}=\hbar v_F/\Delta_0$ for chiral p wave and $\tilde{\xi}=\hbar v_F/|\Delta_0\sin(2\theta_p)|$ for $d+is$- and $d+id$-wave superconductors correspondingly with gap functions given by Eqs. (2) and (3). The spectrum of the Andreev bound states, shifted by the superfluid velocity, is given by

$$\varepsilon_a = \chi\Delta_0 k_y/k_F + \hbar v_{sy} k_y \tag{29}$$

for the p-wave case,

$$\varepsilon_a = \Delta_s \,\mathrm{sgn}(k_y) + \hbar v_{sy} k_y \tag{30}$$

for $d+is$-wave case, and

$$\varepsilon_a = \Delta_d \,\mathrm{sgn}(k_y)\cos(2\theta_p) + \hbar v_{sy} k_y \tag{31}$$

for $d+id$-wave case. Consequently, the contribution from Andreev bound states to the zero-energy LDOS at the surface of a chiral p-wave superconductor is given by

$$N_a = N_0 \frac{1}{|v_{sy}/v_c + \chi|},$$

where $N_0=m/2\pi\hbar^2$ is the normal-metal LDOS per one spin direction. For a chiral $d+is$ superconductor, the behavior of the LDOS is more complicated. Assuming that $\Delta_s>0$, we obtain that the LDOS is zero for $v_{sy}>-\Delta_s/\hbar k_F$. Otherwise, it is given by

$$N_a = 4N_0 \frac{v_{cs} v_c}{v_{sy}^2}.$$

On the contrary, for the $d+id$ case the LDOS is zero if $v_{sy}>\Delta_d/\hbar k_F$ (for $\Delta_d>0$) and otherwise it is given by

$$N_a = N_0 \frac{\Delta_0}{|\Delta_d|}\left(1 + \frac{v_{cd}}{\sqrt{v_{sy}^2 + 8v_{cd}^2}}\right).$$

It can be seen that these contributions to LDOS have peaks at $v_{sy}=v_c$ for p-wave case. For $d+is$-wave and $d+id$-wave superconductors the peaks are positioned at $v_{sy}=-\mathrm{sgn}(\Delta_s)v_{cs}$ and $v_{sy}=\mathrm{sgn}(\Delta_d)v_{cd}$ correspondingly. Even though the position of the peaks are different, the dependencies of the surface LDOS on the superfluid velocity (and consequently on magnetic field) are very similar for $d+is$- and $d+id$-wave superconductors. Therefore, it might be difficult to distinguish which case is realized experimentally.

On the other hand the considered model with a spatially homogeneous gap function $\Psi(\mathbf{r})=1$ is adequate only when the applied magnetic field is not too large. When the magnetic field is large enough, it breaks the Meissner state and generates vortices near the surface of superconductor. Therefore, we investigate the influence of vortices on the LDOS distribution near a superconducting surface as well as on the

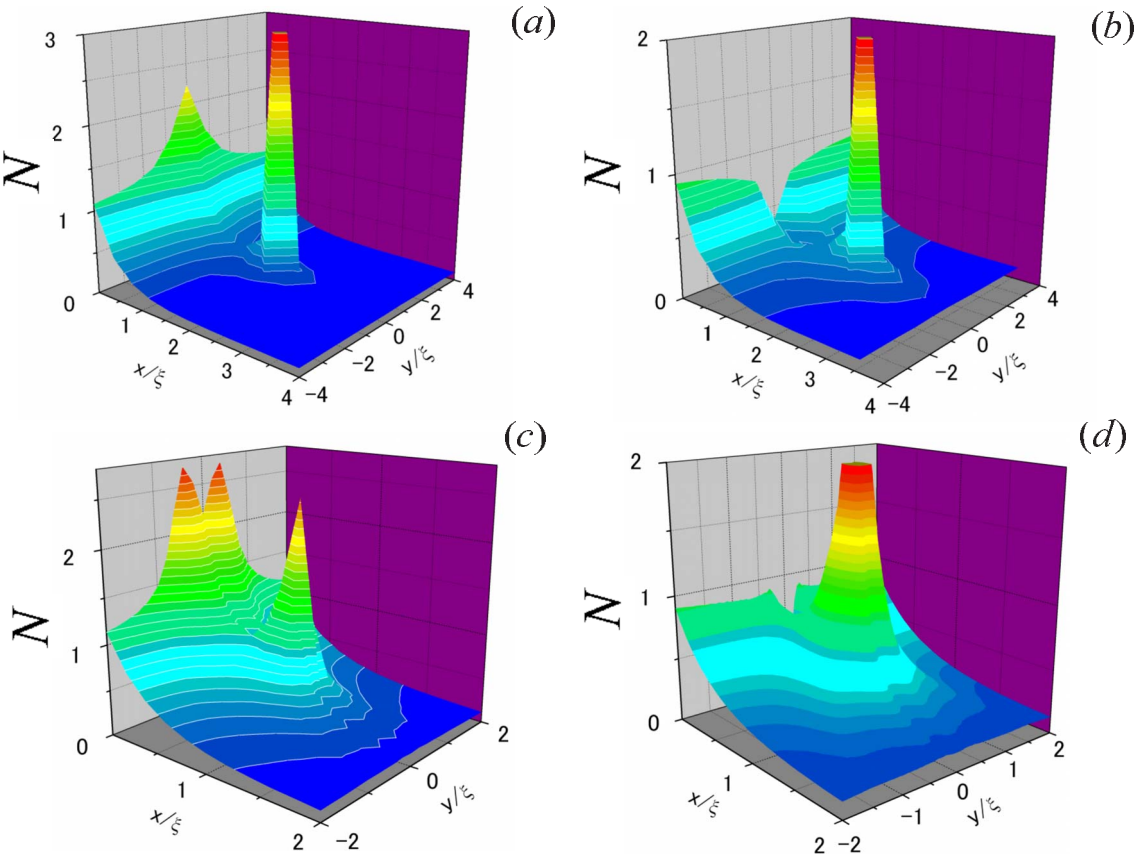

FIG. 4. (Color online) Plot of the normalized zero-energy LDOS $N(0)$ in the presence of a vortex near the surface of a chiral p-wave superconductor. (a) and (c) correspond to equal vorticity and chirality and (b) and (d) correspond to opposite vorticity and chirality. The distance from vortex to the surface is $a=2\xi$ for (a) and (b) and $a=\xi$ for (c) and (d).

conductance of normal-metal/superconducting junctions. We will show that vortices have different effects on the conductance in $d+is$ and $d+id$ cases.

B. Interplay between vortex and surface states in chiral superconductors

A chirality-sensitive LDOS transformation due to vortices situated near the surface of a chiral p-wave superconductor was considered in Ref. 22. It was shown that depending on the chirality and vorticity values, the surface LDOS near is either enhanced or suppressed upon decreasing the distance from the vortex to the surface. In the case of $d+is(d)$ superconductors the transformation of LDOS profile is also sensitive to the value of vorticity. Similar behavior is expected for a conductance of normal-metal/chiral superconductor junction in the presence of vortices.

To investigate the influence of a single vortex on the LDOS profile and conductance, we assume that at $x>0$ (superconducting region) the coordinate dependence of the order parameter may be written as follows:

$$\Psi(\mathbf{r}) = e^{i\Phi}. \tag{32}$$

Here, we consider a model situation where the magnitude of the order parameter is constant. The phase distribution $\Phi(\mathbf{r})$ consists of a singular part $\Phi_v(\mathbf{r})=\arg(\mathbf{r}-\mathbf{r}_v)$ and a regular part $\Phi_r(\mathbf{r})$ determined by the particular metastable vortex lattice configuration realizing near the boundary. We assume that the regular part of the phase distribution is $\Phi_r(\mathbf{r}) = -\arg(\mathbf{r}-\mathbf{r}_{\mathbf{av}})$ corresponding to the image vortex situated at the point $\mathbf{r}_{\mathbf{av}}=(-2a,0,0)$ behind the N/S interface.

1. p+ip wave

In Fig. 4 we show the LDOS profile near the surface of a chiral p-wave superconductor in the presence of a single vortex positioned at some distance a from the surface. When the vortex is positioned far from the surface $a\geq 2\xi$ the LDOS profile follows the behavior, as expected from the picture of local Doppler shift.[22] Depending on the relative values of vorticity and chirality, the surface LDOS is either increased [Fig. 4(a)] or decreased [Fig. 4(b)]. An analytical estimate with the help of spectrum (33) yields the following estimation of the amplitude of LDOS peak in Fig. 4(a): $\Delta N/N_0 = (1+M\chi a)^{-1}$. At smaller distances $a\leq 2\xi$, the behavior of LDOS changes drastically. In the case of opposite vorticity and chirality, the surface LDOS grows at $a\leq 2\xi$, obviously due to the overlapping with the peak of vortex core states. In the case of equal vorticity and chirality the same overlapping occurs, but on the contrary it leads to reduction in DOS, as it was discussed in Sec. I. The peak of the LDOS at the surface discussed in Ref. 22 transforms into a dip-and-peak structure as the vortex comes close to the surface.

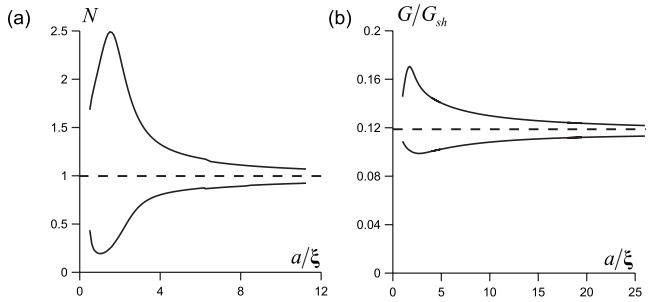

FIG. 5. (a) Plot of the normalized zero-energy LDOS at the point on the surface which is closest to the vortex core. Different curves correspond to different vorticities. (b) Plot of the vortex-induced conductance in chiral $p+ip$-wave superconductor for equal and opposite values of vorticity and chirality. The strength of interface barrier is $Z=5$. Large-distance asymptotes for N and G are shown by dash lines.

This is illustrated in Fig. 5(a), where we plot the LDOS at the surface point (0,0), which is the nearest point to the vortex in Fig. 4. At large distances $a \gg \xi$ the LDOS is a monotonic function of a, either increasing or decreasing depending on the relation between vorticity and chirality. At smaller distances $a \leq 2\xi$, the extremum of LDOS appears. In the case of opposite vorticity and chirality [lower curve in Fig. 5(a)], the surface LDOS grows at $a \leq 2\xi$ due to the overlapping with the peak of vortex core states. In the case of equal vorticity and chirality [upper curve in Fig. 5(a)] the same overlapping leads to reduction in LDOS.

To investigate the influence of vortices on the transport properties of normal-metal/chiral p-wave superconductor junction we solve the generic problem of the influence of a single vortex near the N/S surface on the zero-bias conductance of the junction. A numerical plot of the conductance G as a function of a distance of vortex to the junction interface is shown by the solid lines in Fig. 5(b) for equal (upper curve) and opposite (lower curve) values of chirality and vorticity. The conductance is normalized to the value of Sharvin conductance $G_{\mathrm{Sh}}=k_F L_y/\pi$.

At large distances $a \gg \xi$ an analytical estimation of conductance can be obtained by using a local Doppler-shift approximation on the quasiparticle spectrum. Indeed, the modification of the surface states energy due to a supercurrent flowing along the boundary of superconductor can be written as

$$\varepsilon_a \approx (\chi\Delta_0 + \hbar v_{sy} k_F) k_y/k_F, \tag{33}$$

where k_y is the quasiparticle momentum along the surface, $\chi=\pm 1$ is the chirality value, and $v_{sy}=(M\hbar/m)a/(y^2+a^2)$ is the projection on the surface plane of superfluid velocity generated by the vortex and image antivortex, where M is the vorticity value and m is the electron mass. It follows from Eq. (33) that the Doppler-shift effect leads to a change in the slope of anomalous branch. It is easy to obtain that in this case the function $g(y,\theta_0)$ in expression (22) takes the following form:

$$g(y,\theta_0) = \frac{2}{4(\tilde{Z}^4+\tilde{Z}^2)(\varepsilon_a/\Delta_0)^2+1}. \tag{34}$$

The straightforward integration in Eq. (21) yields $G=G_0+\delta G$, where $G_0=G_{\mathrm{Sh}}(\pi/Z^2)$ is the conductance without vortex and

$$\delta G/G_{\mathrm{Sh}} = \pm \frac{2\pi\xi}{Z^2 L_y} \arctan(L_y/2a) \tag{35}$$

is the vortex-induced conductance shift, where the upper (lower) sign corresponds to equal (opposite) vorticity and chirality.

At distances smaller than 2ξ, an extremum of the conductance appears. Upon placing the vortex closer to the surface, an opposite effect occurs: one obtains a conductance suppression instead of enhancement and vice versa. The origin of the conductance extremum is a tunneling of quasiparticles into the vortex core states or, in other words, the overlapping of vortex and surface-bound states. Comparing Figs. 5(a) and 5(b) one can see that the conductance in general follows the behavior of the surface DOS.

2. d+is and d+id waves

In chiral $d+is$ and $d+id$ superconductors the LDOS transformation appears to also be vorticity sensitive. In Fig. 6 we show the profile of zero-energy LDOS in the case where the vortex is placed at a distance of $a=2\xi$ from a flat boundary of a $d+is$-wave superconductor characterized by a gap function in momentum space given by Eq. (2). In this section, we use the notation $\xi=\hbar v_F/\Delta_0$.

One can see that for one sign of vorticity the surface LDOS shows two peaks which are symmetric with respect to the vortex position. As we have shown above, the large peaks in surface LDOS appear when the energy coincides with the position of bound-state level. For a different sign of the vorticity, there are no surface states at the Fermi level and the LDOS along the surface is a flat function. A nonzero level of LDOS in this case is provided by inelastic scattering which leads to the smearing of the QP energy levels. Applying a local Doppler-shift approach, which holds if the distance from vortex to surface is rather large ($a \gg \xi$), one can interpret the results shown in Fig. 6.

The coordinates y^* of surface LDOS peaks can be estimated from the relation $v_{sy}=\Delta_s/p_F$, where $v_{sy}=(M\hbar/m)a/(y^2+a^2)$ is the projection on the surface plane of superfluid velocity generated by the vortex with vorticity M and image antivortex. It can be seen that for $a>\xi(\Delta_0/|\Delta_s|)$ the peak is situated at $y^*=0$, i.e., at the surface point nearest to the vortex. Otherwise, we obtain $y^*=\pm a\sqrt{1-(a/\xi)(|\Delta_s|/\Delta_0)}$. Comparing this estimation with the numerical results in Fig. 6, one observes a minor difference. For example, it follows from the estimation that the LDOS peaks should be positioned at $y^*=\pm 2.4\xi$ for $\Delta_s=0.2\Delta_0$, but in Fig. 6 they are located at $y^*=\pm 2.0\xi$. This discrepancy can be attributed to the complex shift of the energy $\varepsilon \to \varepsilon + i\delta$ due to the effective scattering parameter $\delta=0.1\Delta_0$ which was

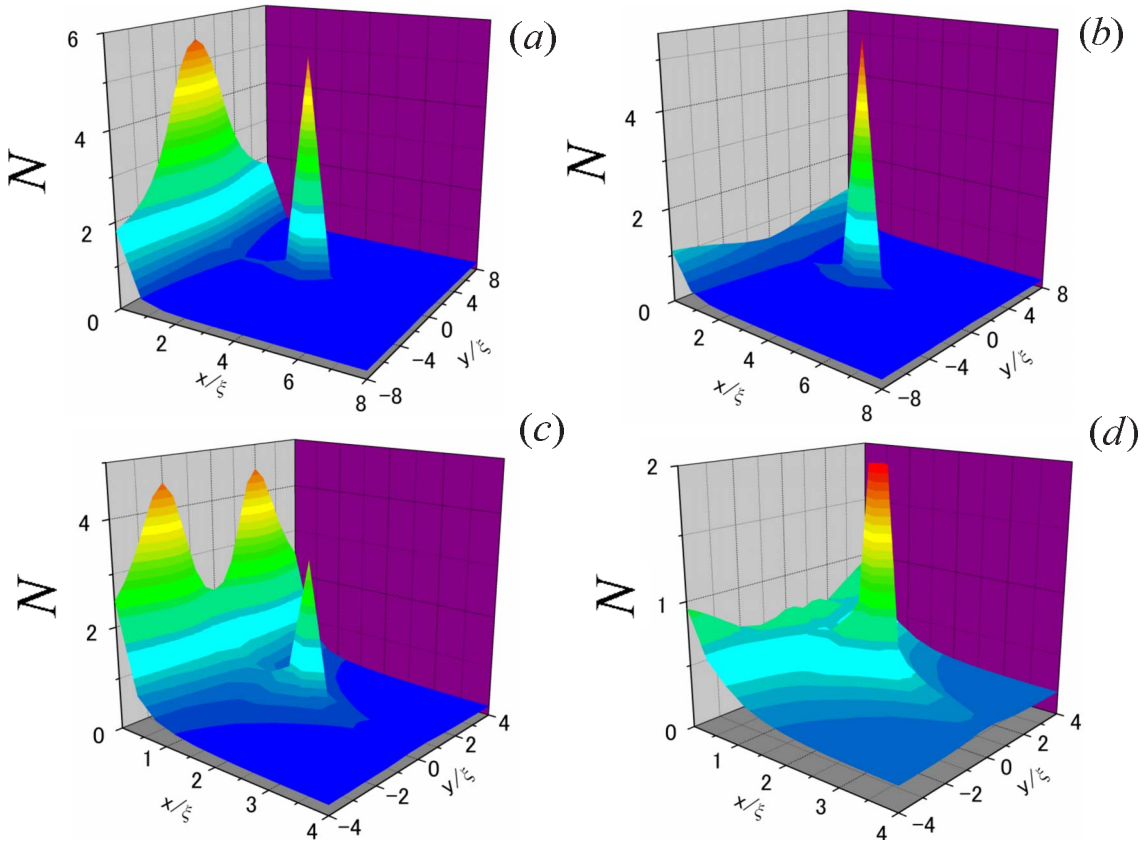

FIG. 6. (Color online) Plot of the normalized zero-energy LDOS profile $N(0)$ in the presence of vortex near the surface of chiral $d+is$-wave superconductor with $\Delta_s=0.2\Delta_0$. (a)–(d) correspond to different vortex orientations with respect to the z axis. The distance from vortex to the surface is $a=4\xi$ for (a) and (b) and $a=2\xi$ for (c) and (d).

used in the numerical calculations. If we increase the distance from vortex to surface, a, the LDOS peaks will merge when $a>\xi(\Delta_0/|\Delta_s|)$ (see Fig. 6).

In Fig. 7, we show the LDOS profile modulated by a vortex placed at a distance of $a=2\xi$ from a flat boundary of $d+id$ superconductor. The structure of the gap function was chosen in the form (3). Applying the approach based on the local Doppler shift we obtain the similar expression for the coordinates of the peaks of surface LDOS: $y^*=\pm a\sqrt{1-(a/\xi)(|\Delta_d|/\Delta_0)}$. For the particular values of parameters $\Delta_d=0.2\Delta_0$ and $a=2\xi$ this estimation yields $y^*=\pm 2.4\xi$, which is much less than obtained from numerical plot in Fig. 7 ($y^*\approx\pm 4\xi$). This discrepancy can also be attributed to the effect of inelastic scattering, which appears to have a larger effect in $d+id$-wave case than in discussed above $d+is$-wave case.

A numerical plot of the N/S junction conductance as a function of distance from vortex to surface is shown in Fig. 8 for the $d+is$ and $d+id$ cases. The conductance is normalized to the Sharvin conductance $G_{\mathrm{Sh}}=k_F L_y/\pi$. Comparing Figs. 8(a) and 8(b) one can see that the conductance behavior is qualitatively different for s- and d-wave symmetries of the additional gap function component. For $d+is$ wave, the conductance has a sharp peak for one vortex orientation [upper curve in Fig. 8(a)] and it is a flat function of a for another vortex orientation [lower curve in Fig. 8(a)]. The origin of the conductance enhancement is a formation of Andreev bound states at the Fermi level which are localized near the superconducting surface. As was discussed in Sec. I [see Fig. 1(b)], the zero-energy Andreev bound states can appear only for a certain direction of superfluid velocity flowing along the superconducting surface and if the value of the superfluid velocity is larger than a critical value $|v_{sy}|>|\Delta_s|/\hbar k_F$. For a high interface barrier $Z\gg 1$, applying the approximate analytical expression (35), we find that a sharp increase in conductance in Fig. 8(a) can be described by the following expression:

$$G/G_{\mathrm{Sh}}=\frac{16\pi}{3Z^2}\frac{\xi}{L_y}\frac{\Delta_0}{|\Delta_s|}\left(1-\frac{a}{a^*}\right)^{3/2}+\lambda Z^{-4},$$

where $a^*=\xi(\Delta_0/|\Delta_s|)$ and $\lambda\sim 1$. Otherwise, if $a>a^*$ the conductance is much smaller since $Z\gg 1$,

$$G/G_{\mathrm{Sh}}\approx\left(\frac{\Delta_0}{\Delta_s}\right)^2\frac{4}{3Z^4}.$$

When the distance a is decreased further, the conductance is suppressed [see Fig. 8(a), upper curve]. The decrease in conductance can be attributed to the gap at the Fermi level which appears due to the interaction of vortex and surface states in a similar way as for the $p+ip$-wave case discussed in Sec. III B 1.

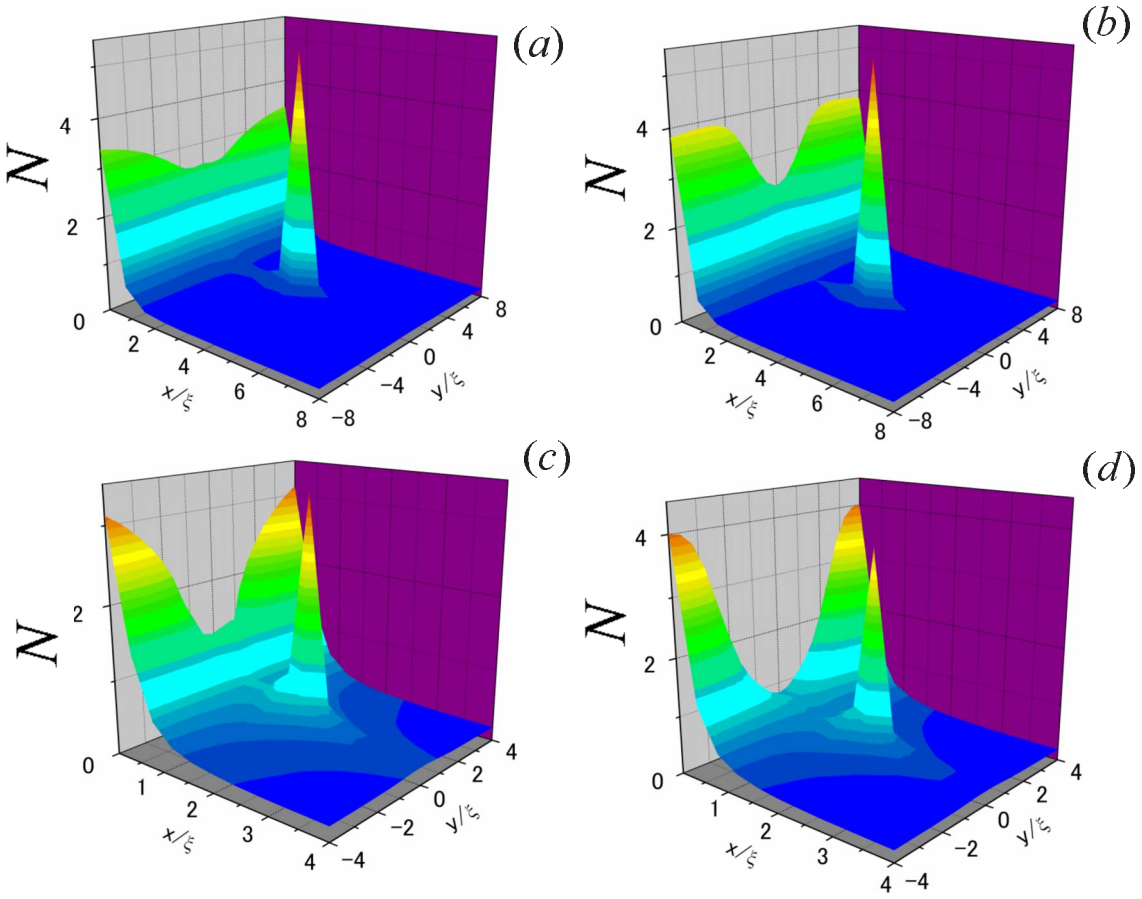

FIG. 7. (Color online) Plot of the normalized zero-energy LDOS profile $N(0)$ in the presence of vortex near the surface of chiral $d+id$-wave superconductor with $\Delta_d=0.2\Delta_0$ (a)–(d) correspond to different vortex orientations with respect to the z axis. The distance from vortex to the surface is $a=4\xi$ for (a) and (b) and $a=2\xi$ for (c) and (d).

In a $d+id$-wave superconductor, zero-energy Andreev bound states may exist even in the absence of vortex. An asymptotic value of the conductance G_0 at $a \gg \xi$ can be obtained using expression (35) as follows:

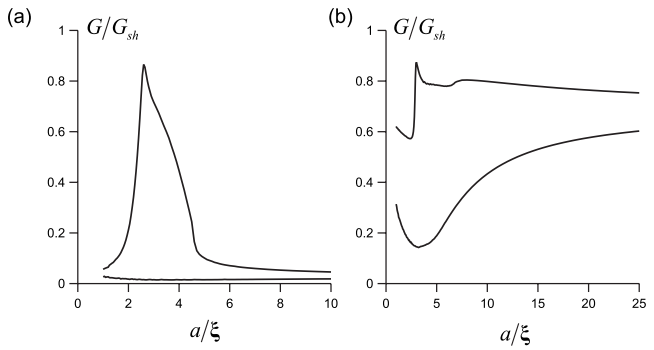

FIG. 8. Plots of the vortex-induced conductance in cases of (a) chiral $d+is$ superconductor for $\Delta_s=0.2\Delta_0$ and (b) $d+id$ superconductor for $\Delta_d=0.2\Delta_0$. The strength of interface barrier is $Z=5$. Different curves on each plot correspond to different vortex orientations with respect to the z axis.

$$G_0/G_{\mathrm{Sh}} = \left(\frac{\Delta_0}{|\Delta_d|}\right)\frac{\pi}{2\sqrt{2}Z^2}.$$

When the vortex approaches the superconducting surface, the conductance is either suppressed [lower curve in Fig. 8(b)] or slightly enhanced [upper curve in Fig. 8(b)]. This behavior can be understood by again using the Eq. (35) with the Doppler-shifted spectrum of Andreev bound states (6). The decrease (increase) in conductance corresponds to the transformation of spectrum shown qualitatively in Fig. 1(c) by dashed (dashed-dotted) lines. It is possible to obtain an analytical expression for the vortex-induced conductance shift at $a \gg \xi$ in the following form:

$$\delta G/G_{\mathrm{Sh}} = \pm\frac{\pi}{2Z^2}\left(\frac{\Delta_0}{\Delta_d}\right)^2\frac{\xi}{L_y}\arctan\left(\frac{L_y}{2a}\right),$$

where the upper and lower signs correspond to the different vortex orientations. As the vortex approaches the surface further, there appears an extremum of the conductance. Such behavior can be explained by a conductance enhancement due to the tunneling of QP into the vortex core states discussed in Ref. 32. A sharp decrease in the upper curve in Fig. 8(b) can be attributed to the opening of an energy gap at the

Fermi level due to the interaction of vortex and surface states.

IV. SUMMARY

In summary, we have investigated how the tunneling conductance and the local density of states (LDOS) in superconductors are affected by the influence of an external magnetic field when the superconducting OP breaks TRS. This is directly relevant for both Sr_2RuO_4, where chiral $p+ip$-wave pairing is believed to be realized, and for the high-T_c cuprates, where a $d+is$- or $d+id$-wave OP has been suggested to exist near surfaces. In addition to breaking TRS, all of these OPs feature surface-bound zero-energy states at surfaces under appropriate circumstances (e.g., a dominant d-wave OP in the $d+is$-wave case).

We have shown how the Doppler shift conspires with an interaction of vortex and surface states to produce a considerable qualitative modification of both the tunneling conductance and the LDOS. When the vortex is located at distances well above a coherence length ξ from the surface, the Doppler shift produces an enhancement or suppression of the LDOS depending on the relative sign of the vorticity and the chirality of the superconducting OP. This effect may be directly probed by first applying an external magnetic field in a direction while measuring the LDOS and then reversing the field direction and measuring again. When the vortex is located very close to the surface (a distance on the order of ξ or smaller), there is an overlap between the vortex and surface states which effectively causes a dramatic change in the tunneling conductance and LDOS. This effect is also sensitive to the relative signs of the vorticity and the chirality of the superconducting OP. The overlap between these two sets of states results in either a strongly enhanced or suppressed tunneling conductance/LDOS at zero-bias voltage/zero energy.

We have demonstrated the aforementioned effects both qualitatively and quantitatively for $p+ip$-, $d+is$-, and $d+id$-wave symmetries. Experimentally, the distance from the surface to the closest vortex can be altered by modifying the field strength. All of our predictions should be possible to test experimentally with present-day techniques.

ACKNOWLEDGMENTS

M.A.S. is grateful to Alexander S. Mel'nikov for numerous stimulating discussions. This work was supported in part by Russian Foundation for Basic Research, by Program "Quantum Macrophysics" of RAS, and by Russian Science Support and "Dynasty" Foundations. J.L. and A.S. were supported by the Norwegian Research Council Grants No. 158518/431, No. 158547/431 (NANOMAT), and No. 167498/V30 (STORFORSK). T.Y. acknowledges the support by JSPS.

[1] Y. Maeno, H. Hashimoto, K. Yoshida, S. Nishizaki, T. Fujita, J. G. Bednorz, and F. Lichtenberg, Nature (London) **372**, 532 (1994); K. Ishida, H. Mukuda, Y. Kitaoka, K. Asayama, Z. Q. Mao, Y. Mori, and Y. Maeno, *ibid.* **396**, 658 (1998); G. M. Luke, Y. Fudamoto, K. M. Kojima, M. I. Larkin, J. Merrin, B. Nachumi, Y. J. Uemura, Y. Maeno, Z. Q. Mao, Y. Mori, H. Nakamura, and M. Sigrist, *ibid.* **394**, 558 (1998); A. P. Mackenzie and Y. Maeno, Rev. Mod. Phys. **75**, 657 (2003); K. D. Nelson, Z. Q. Mao, Y. Maeno, and Y. Liu, Science **306**, 1151 (2004); Y. Asano, Y. Tanaka, M. Sigrist, and S. Kashiwaya, Phys. Rev. B **67**, 184505 (2003); **71**, 214501 (2005).

[2] L. J. Buchholtz, M. Palumbo, D. Rainer, and J. A. Sauls, J. Low Temp. Phys. **101**, 1079 (1995).

[3] M. Matsumoto and H. Shiba, J. Phys. Soc. Jpn. **64**, 3384 (1995).

[4] K. Kuboki and M. Sigrist, J. Phys. Soc. Jpn. **65**, 361 (1996).

[5] M. Sigrist, Prog. Theor. Phys. **99**, 899 (1998).

[6] L. J. Buchholtz, M. Palumbo, D. Rainer, and J. A. Sauls, J. Low Temp. Phys. **101**, 1099 (1995).

[7] M. Matsumoto and H. Shiba, J. Phys. Soc. Jpn. **64**, 4867 (1995).

[8] M. Fogelstrom, D. Rainer, and J. A. Sauls, Phys. Rev. Lett. **79**, 281 (1997).

[9] Y. Tanuma, Y. Tanaka, M. Ogata, and S. Kashiwaya, J. Phys. Soc. Jpn. **67**, 1118 (1998); Phys. Rev. B **60**, 9817 (1999).

[10] M. Covington, M. Aprili, E. Paraoanu, L. H. Greene, F. Xu, J. Zhu, and C. A. Mirkin, Phys. Rev. Lett. **79**, 277 (1997); A. Biswas, P. Fournier, M. M. Qazilbash, V. N. Smolyaninova, H. Balci, and R. L. Greene, *ibid.* **88**, 207004 (2002); Y. Dagan and G. Deutscher, *ibid.* **87**, 177004 (2001); A. Sharoni, O. Millo, A. Kohen, Y. Dagan, R. Beck, G. Deutscher, and G. Koren, Phys. Rev. B **65**, 134526 (2002); A. Kohen, G. Leibovitch, and G. Deutscher, Phys. Rev. Lett. **90**, 207005 (2003); M. Aprili, E. Badica, and L. H. Greene, *ibid.* **83**, 4630 (1999); R. Krupke and G. Deutscher, *ibid.* **83**, 4634 (1999).

[11] M. Franz and Z. Tesanovic, Phys. Rev. Lett. **80**, 4763 (1998).

[12] C. R. Hu, Phys. Rev. Lett. **72**, 1526 (1994).

[13] J. Yang and C.-R. Hu, Phys. Rev. B **50**, 16766 (1994).

[14] Y. Tanaka and S. Kashiwaya, Phys. Rev. Lett. **74**, 3451 (1995); S. Kashiwaya and Y. Tanaka, Rep. Prog. Phys. **63**, 1641 (2000).

[15] J. Y. T. Wei, N. C. Yeh, D. F. Garrigus, and M. Strasik, Phys. Rev. Lett. **81**, 2542 (1998).

[16] Z. Q. Mao, K. D. Nelson, R. Jin, Y. Liu, and Y. Maeno, Phys. Rev. Lett. **87**, 037003 (2001).

[17] L. Alff, S. Kleefisch, U. Schoop, M. Zittartz, T. Kemen, T. Bauch, A. Marx, and R. Gross, Eur. Phys. J. B **5**, 423 (1998); H. Walter, W. Prusseit, R. Semerad, H. Kinder, W. Assmann, H. Huber, H. Burkhardt, D. Rainer, and J. A. Sauls, Phys. Rev. Lett. **80**, 3598 (1998); Yu. S. Barash, M. S. Kalenkov, and J. Kurkija¨rvi, Phys. Rev. B **62**, 6665 (2000); A. Carrington, F. Manzano, R. Prozorov, R. W. Giannetta, N. Kameda, and T. Tamegai, Phys. Rev. Lett. **86**, 1074 (2001).

[18] Y. Tanaka and S. Kashiwaya, Phys. Rev. B **53**, R11957 (1996); Yu. S. Barash, H. Burkhardt, and D. Rainer, Phys. Rev. Lett. **77**, 4070 (1996); R. A. Riedel and P. F. Bagwell, Phys. Rev. B **57**, 6084 (1998); E. Il'ichev, M. Grajcar, R. Hlubina, R. P. J. IJsselsteijn, H. E. Hoenig, H. G. Meyer, A. Golubov, M. H. S. Amin, A. M. Zagoskin, A. N. Omelyanchouk, and M. Y. Kupriyanov,

Phys. Rev. Lett. **86**, 5369 (2001).
[19] Yu. S. Barash, A. M. Bobkov, and M. Fogelstrom, Phys. Rev. B **64**, 214503 (2001).
[20] S. Graser, C. Iniotakis, T. Dahm, and N. Schopohl, Phys. Rev. Lett. **93**, 247001 (2004).
[21] C. Iniotakis, S. Graser, T. Dahm, and N. Schopohl, Phys. Rev. B **71**, 214508 (2005).
[22] T. Yokoyama, C. Iniotakis, Y. Tanaka, and M. Sigrist, Phys. Rev. Lett. **100**, 177002 (2008).
[23] N. B. Kopnin and G. E. Volovik, JETP Lett. **64**, 690 (1996).
[24] Y. Morita, M. Kohmoto, and K. Maki, Phys. Rev. Lett. **78**, 4841 (1997).
[25] M. Franz and Z. Tesanovic, Phys. Rev. Lett. **87**, 257003 (2001); O. Vafek, A. Melikyan, M. Franz, and Z. Tesanovic, Phys. Rev. B **63**, 134509 (2001); O. Vafek, A. Melikyan, and Z. Tesanovic, *ibid.* **64**, 224508 (2001); A. Melikyan and Z. Tesanovic, *ibid.* **76**, 094509 (2007).
[26] A. S. Mel'nikov, Phys. Rev. Lett. **86**, 4108 (2001).
[27] M. Tinkham, *Introduction to Superconductivity*, 2nd ed. (McGraw-Hill, New York, 1996), Chap. 10.
[28] J. Goryo and M. Sigrist, J. Phys.: Condens. Matter **12**, L599 (2000).
[29] G. E. Volovik, JETP Lett. **70**, 609 (1999).
[30] C. Caroli, P. G. de Gennes, and J. Matricon, Phys. Lett. **9**, 307 (1964).
[31] N. B. Kopnin, Phys. Rev. B **57**, 11775 (1998).
[32] M. A. Silaev, Phys. Rev. B **77**, 014504 (2008).
[33] J. Bardeen, R. Kummel, A. E. Jacobs, and L. Tewordt, Phys. Rev. **187**, 556 (1969).
[34] G. D. Mahan, *Many-Particle Physics*, 2nd ed. (Plenum, New York, 1993), Chap. 9.
[35] T. Dahm, S. Graser, C. Iniotakis, and N. Schopohl, Phys. Rev. B **66**, 144515 (2002).
[36] N. Schopohl and K. Maki, Phys. Rev. B **52**, 490 (1995); N. Schopohl, arXiv:cond-mat/9804064 (unpublished).
[37] G. E. Blonder, M. Tinkham, and T. M. Klapwijk, Phys. Rev. B **25**, 4515 (1982).
[38] R. Krupke and G. Deutscher, Phys. Rev. Lett. **83**, 4634 (1999).
[39] A. Sharoni, G. Koren, and O. Millo, Europhys. Lett. **54**, 675 (2001).